

Analysis of the high Reynolds number 2D tests on a wind turbine airfoil performed at two different wind tunnels

This content has been downloaded from IOPscience. Please scroll down to see the full text.

2016 J. Phys.: Conf. Ser. 749 012014

(<http://iopscience.iop.org/1742-6596/749/1/012014>)

View [the table of contents for this issue](#), or go to the [journal homepage](#) for more

Download details:

IP Address: 130.112.1.3

This content was downloaded on 21/02/2017 at 11:24

Please note that [terms and conditions apply](#).

Analysis of the high Reynolds number 2D tests on a wind turbine airfoil performed at two different wind tunnels

O Pires¹, X Munduate¹, O Ceyhan², M Jacobs³, J Madsen⁴ and J G Schepers²

¹ National Renewable Energy Centre (CENER), 31621 Sarriguren, Navarra, Spain

² Energy Research Center of the Netherlands (ECN), 1755LE, Petten, The Netherlands

³ DNW, Bunsenstrasse 10, 37073 Göttingen, Germany

⁴ LM Wind Power, Lunderskov, Denmark

E-mail: oepires@cener.com

Abstract. 2D wind tunnel tests at high Reynolds numbers have been done within the EU FP7 AVATAR project (AdVanced Aerodynamic Tools of lArge Rotors) on the DU00-W-212 airfoil and at two different test facilities: the DNW High Pressure Wind Tunnel in Gottingen (HDG) and the LM Wind Power in-house wind tunnel. Two conditions of Reynolds numbers have been performed in both tests: 3 and 6 million. The Mach number and turbulence intensity values are similar in both wind tunnels at the 3 million Reynolds number test, while they are significantly different at 6 million Reynolds number. The paper presents a comparison of the data obtained from the two wind tunnels, showing good repeatability at 3 million Reynolds number and differences at 6 million Reynolds number that are consistent with the different Mach number and turbulence intensity values.

1. Introduction

Within the EU FP7 AVATAR project (AdVanced Aerodynamic Tools of lArge Rotors) [1], 2D tests have been performed at high Reynolds numbers in order to evaluate airfoil performance under the expected conditions of the future multi-MW wind turbine blades. The DU00-W-212, a 21% relative thickness airfoil from the TU-Delft DU airfoil family, has been tested at the DNW High Pressure Wind Tunnel in Göttingen (HDG) at 5 different Reynolds numbers (3, 6, 9, 12 and 15 million) and low Mach numbers (below 0.1). In parallel, LM Wind Power has performed at his own wind tunnel facility a test on this same airfoil at two different Reynolds numbers, 3 and 6 million, and Mach numbers of 0.14 and 0.28 respectively.

The comparison of the results from these two experiments gives a good opportunity to check the repeatability of the results of airfoil aerodynamic performance data when obtained at different facilities. In addition, the effect of significant differences in Mach number and turbulence intensity conditions can be observed on the airfoil aerodynamic coefficients behavior.

2. Tests description

Both wind tunnel tests have been performed on a 2D model of the DU00-W-212 airfoil arranged horizontally in a closed test section. The models were instrumented with 90 pressure taps to capture



the static pressure distribution around the airfoil and a wake rake downstream to measure the total pressure of the wake. Lift and pitching moment coefficients (C_l and C_m) were obtained by integration of the pressure distribution around the airfoil and Drag coefficient (C_d) was calculated from the wake loss of momentum by integrating the wake total pressure distribution.

A description of each of the wind tunnel facilities and their particular test arrangement is presented below:

2.1. DNW wind tunnel test

The DNW HDG is a closed return circuit wind tunnel with a closed test section of 0.6 x 0.6 m. (width x height) and 1 m. length, and a contraction ratio of 5.85. The wind tunnel speed range is 3.5 to 35 m/s and the maximum Mach number is 0.1. This tunnel can be pressurized up to 100 bars to achieve high Reynolds numbers.

A 150 mm. chord 2D airfoil model was horizontally installed in the middle of the test section and was equipped with 90 pressure taps at the mid span. A wake rake with 118 total and 8 static pressure probes was installed around 2 chords downstream of the trailing edge of the model.

The data presented in this paper has been corrected using classical wind tunnel wall corrections compiled in AGARD-AG-336 [2].

Tests have been performed at different Reynolds numbers: 3, 6, 9, 12 and 15 million. Analysis of the Reynolds effect on the airfoil performance has been reported in [3]. Measurements have been performed at airfoil surface clean configuration as well as with transition dots installed in the model to force laminar to turbulent boundary layer transition at a certain chord position.

Additional instrumentation as a 3-component balance for correlation of the aerodynamic coefficients, 5 fast response kulite sensors installed in the model for unsteady pressure measurements, a cylindrical hot-film probe for inflow speed fluctuation measurements and UV LED light and camera for oil flow visualization have also been used.

2.2. LM wind tunnel test

LM wind tunnel is an atmospheric closed return circuit wind tunnel with a closed test section of 1.35 x 2.7 m. (width x height) and 7 m. length, and a contraction ratio of 10. The maximum wind speed at the test section is 105 m/s.

A 900 mm. chord 2D airfoil model instrumented with 90 pressure taps was horizontally installed in the test section. A wake rake instrumented with total and static pressure probes is installed downstream of the model.

All the data presented here has been corrected for wind tunnel effects classical wind tunnel wall corrections as described in standards given in AGARD-AG-336 [2]

Tests have been performed at two Reynolds numbers conditions, 3 and 6 million. Measurements have been done at airfoil surface clean configuration as well as with transition zig-zag tape installed in the model to force the laminar to turbulent boundary layer transition. In addition, some configurations with vortex generators and gurney flaps have been tested. An analysis of the effect of these configurations has been reported within the AVATAR project.

Some additional instrumentation was also used in this test, as floor and ceiling pressure holes distributions along the centerline of the test section and a load cell system for measuring the airfoil lift, drag and pitching moment coefficients.

2.3. Main differences between both tests

Both tests have been done over the same airfoil geometry and using the same methodology for obtaining the aerodynamic coefficients. The instrumentation of the model was also done in the same way for both experiments, using the same number and chord-wise positions of the pressure taps.

However, there are some differences between both experiments that have to be taken into account when comparing the results. These main differences can be summarized, on one hand in the geometric

set up of the models and test sections, and on the other in the different wind conditions reproduced in the test section.

From the geometric differences shown in Table 1, it can be seen how the model chord size in the HDG test is 6 times smaller than in the LM test. This should not have to make any difference in the results, but it has to be considered for the test arrangement as in a small model the height of forcing transition elements has to be smaller as well. In this way, to assure the laminar boundary layer behavior in the clean configuration cases, a good surface treatment of the model has to be made, and in the case of the HDG model, the surface roughness was set always below $R_z 0.1 \mu\text{m}$.

The model aspect ratio (ratio between span and chord of the model) difference between both experiments is also considerable, being 2.6 times bigger in the case of the HDG. This difference will affect the 3-dimensional effects that appear in the tests. These effects are mostly important when separation phenomena occur.

The geometric blockage parameter is presented as it gives an indication of the tunnel test section wall effects and therefore the order of wall interference tunnel corrections applied. For both tests, the parameter is similar and low enough to derive reliable wind tunnel wall corrections up to angles of attack (AoA) of 20° .

Table 1. Geometric set up differences between the two experiments

	HDG	LM
Test section (W x H)	0.6 m x 0.6 m	1.35 m x 2.7 m
Model span (S)	0.6 m	1.35 m
Model chord (c)	0.15 m	0.9 m
Model aspect ratio (S/c)	4	1.5
Geometric blockage (c/H)	25%	33%

The other important differences between the tests are the airflow conditions. Table 2 shows the Mach number and the Turbulence intensity for the two Reynolds number conditions that are being analysed in this paper, 3 and 6 million. The turbulence intensity (TI) is lower at LM. This could affect in principle the laminar behavior of the airfoil.

The Mach number shows important differences between the tests. The reason is that in the DNW test, the Reynolds number variation is obtained modifying the air density by pressurizing the wind tunnel airflow. Therefore the Mach number is always maintained low (below 0.1) and only a pure Reynolds number variation is obtained. On the other hand, in the LM test the Reynolds number variation is obtained modifying the wind speed and therefore the Mach number. We can see then, that for the Reynolds number 3 million condition the Mach number for both tests is similar (around 0.1). But for the Reynolds number 6 million, the LM test has a Mach number one order of magnitude greater than HDG and close to 0.3. So, compressible effects could be observed between those tests at these conditions.

Table 2. Wind condition differences between the two experiments

	Reynolds 3million test		Reynolds 6 million test	
	HDG	LM	HDG	LM
Mach number (M)	0.08	0.139	0.03	0.279
Turbulence intensity (TI)	0.1 %	0.05 %	0.2 %	0.1 %

3. Data comparison between both tests

A comparison of the results obtained in both tests is presented below. The lift coefficient (C_l) against angle of attack (AoA) and against drag coefficient (C_d), and the efficiency (C_l/C_d) against angle of attack have been plotted for the Reynolds number 3 million case and for the 6 million one.

3.1. Reynolds 3 million comparison

Figure 1 shows the comparison between both tests of the lift curve against angle of attack. The curves match very well in the linear region and even at the maximum C_l value.

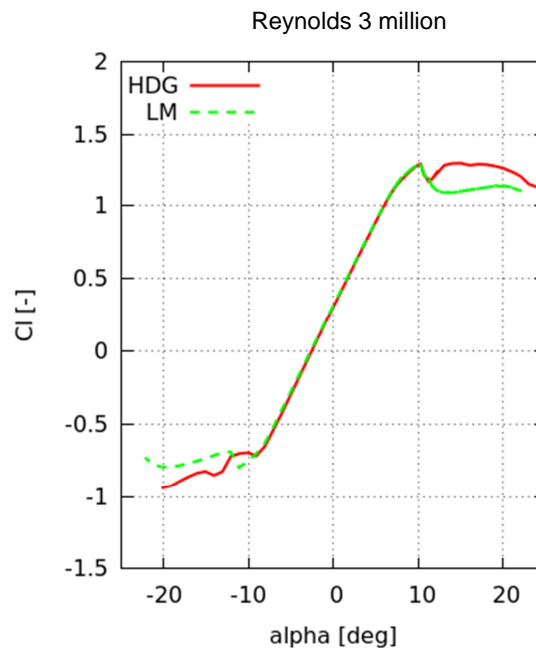


Figure 1. Lift coefficient (C_l) vs angle of attack (AoA) comparison at $Re=3 \cdot 10^6$

Only different behavior is observed at the stall condition, where 3D effects can be greatly affected by formation of stall cells, whose size and number are influenced by the aspect ratio of the model [5]. The span-wise position of the pressure taps also influences the measured lift, as the level of separated flow measured by the tap depends on the typology of the stall cells created. An example of this phenomenon can be seen on Figure 2.

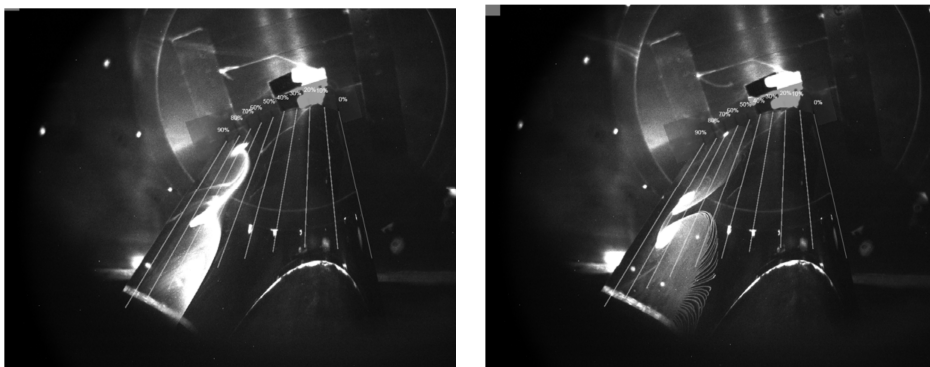


Figure 2. DNW flow visualization photos at 14° AoA (left) and 18° AoA (right)

Figure 2 shows two pictures from the flow visualization performed at the DNW test. They correspond to two different post stall angles of attack. The pictures show the model from a window on the starboard wall of the test section. Some white lines are superimposed on the pictures to show different chord-wise positions (the most right one corresponds to the leading edge of the model). As it can be seen in the pictures, the topology of the stall cells varies with the angles of attack and produces different levels of chord percentage of the model being stalled depending on the span position. Therefore, the positioning of the pressure taps influences the measured lift.

The differences in lift in the stall region between both tests can then be explained with the different aspect ratio of the model.

The measured drag matches also very well in the linear region. Figure 3 shows how the drag bucket is completely reproduced in shape and values. Since both lift and drag are well reproduced, it is expected that the airfoil efficiency (lift over drag ratio) will be also similar. We can also observe this in Figure 4.

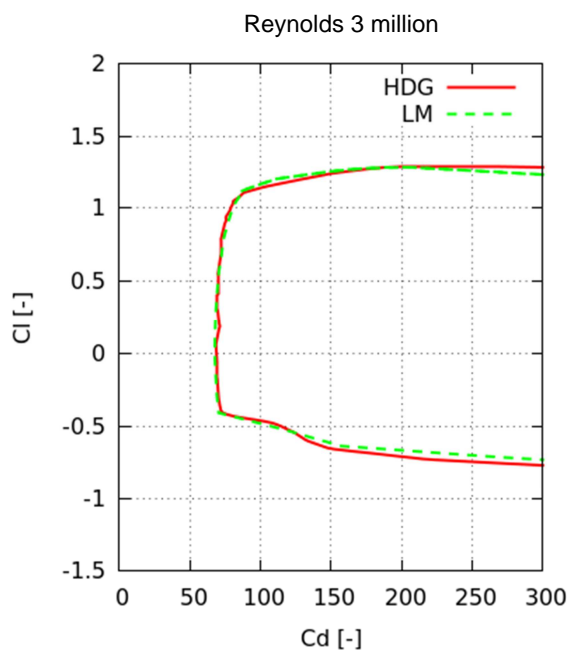


Figure 3. Cl vs Cd comparison at $Re=3 \cdot 10^6$

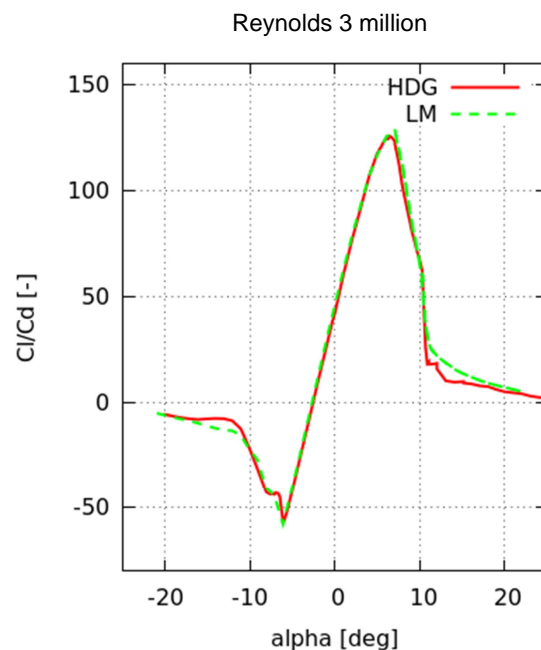


Figure 4. Cl/Cd comparison at $Re=3 \cdot 10^6$

3.2. Reynolds 6 million comparison

When we look into the data at Reynolds number 6 million, we can see that in this case the results from both tests do not show such a good agreement. We can already see in Figure 5 how the lift slope is different and greater in the data from LM test. The drag values keep a very good comparison in the linear region but the bucket corners (as it can be seen in Figure 6) are different, indicating a different behavior on the boundary layer laminar to turbulent transition and separation.

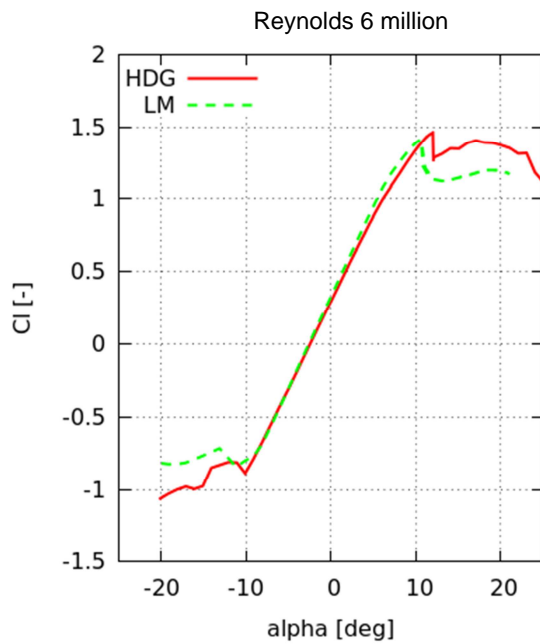


Figure 5. Cl vs AoA comparison at $Re=6 \cdot 10^6$

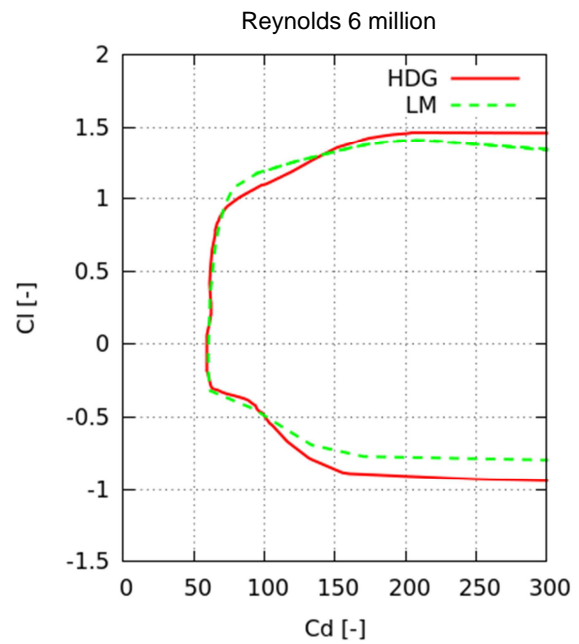


Figure 6. Cl vs Cd comparison at $Re=6 \cdot 10^6$

Attending to these differences between lift and drag, the efficiency curve shows the worst agreement in the maximum values (Figure 7), as LM results have a greater lift due to its higher slope and a lower drag in the upper bucket corner.

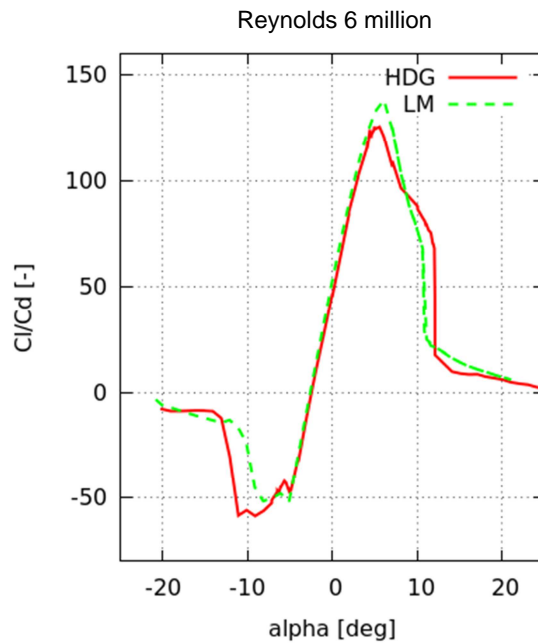


Figure 7. Cl/Cd comparison at $Re=6 \cdot 10^6$

4. Analysis of the effect of the Mach number and turbulence intensity

The next step is to study the reason for obtaining different comparison results at each Reynolds number. We look therefore to tables 1 and 2 to see the differences we have at each condition. The set-up differences listed at table 1 are the same for both Reynolds. Although their effect on the results could have some variability depending on Reynolds, they affect mainly the results when separation occurs, at high angles of attack, as it has been already discussed. Table 2 shows different wind conditions at each Reynolds number. The turbulence is in both cases twice at HDG. From this different air stream turbulence, it is mainly expected to have a different measurement in drag.

The Mach number has the same order of magnitude for the Reynolds 3 million case, but for the Reynolds 6 million case is one order of magnitude higher at LM.

The higher slope of the lift coefficient is compatible with higher Mach number. If we make a simplified compressible correction using Prandtl-Glauert law [4], expressed in (1) on the HDG data to obtain the values that would be expected at a Mach number (M_∞) of 0.279, we see in Figure 8 that the linear region would match.

$$C_l = \frac{C_{l,0}}{\sqrt{1-M_\infty^2}} \quad \text{where } C_{l,0} \text{ is the lift coefficient for the incompressible flow } (M_\infty=0) \quad (1)$$

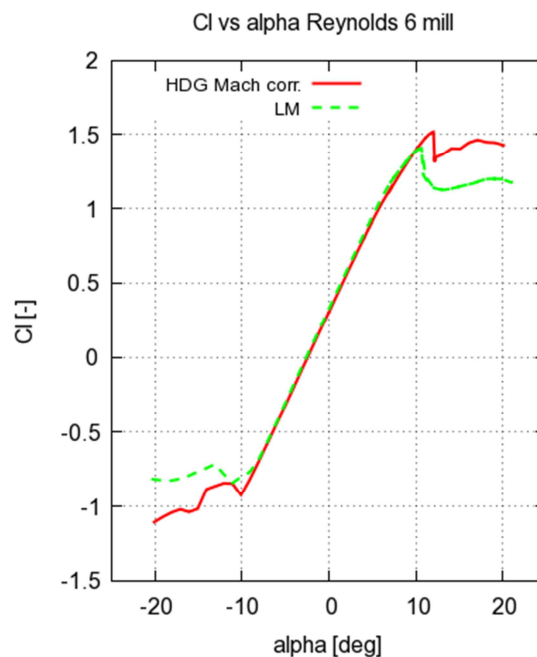


Figure 8. Lift comparison between both tests applying Prandtl-Glauert compressibility correction to HDG data

The differences in the maximum lift could be explained by the Mach effect, as the Prandtl-Glauert law is only valid for the C_l linear region, but they can also be explained by the different 3D effects created by the stall cell formations [6].

An analysis using the panel method code XFOIL version 6.96 has been performed to evaluate the differences we can expect by modifying Mach number and inflow turbulence. In Figure 9, Figure 10 and Figure 11, the experimental differences for Reynold number 6 million case (at the left) are compared to computations differences when Mach number and N-factor (from the e^N method for transition prediction) are modified.

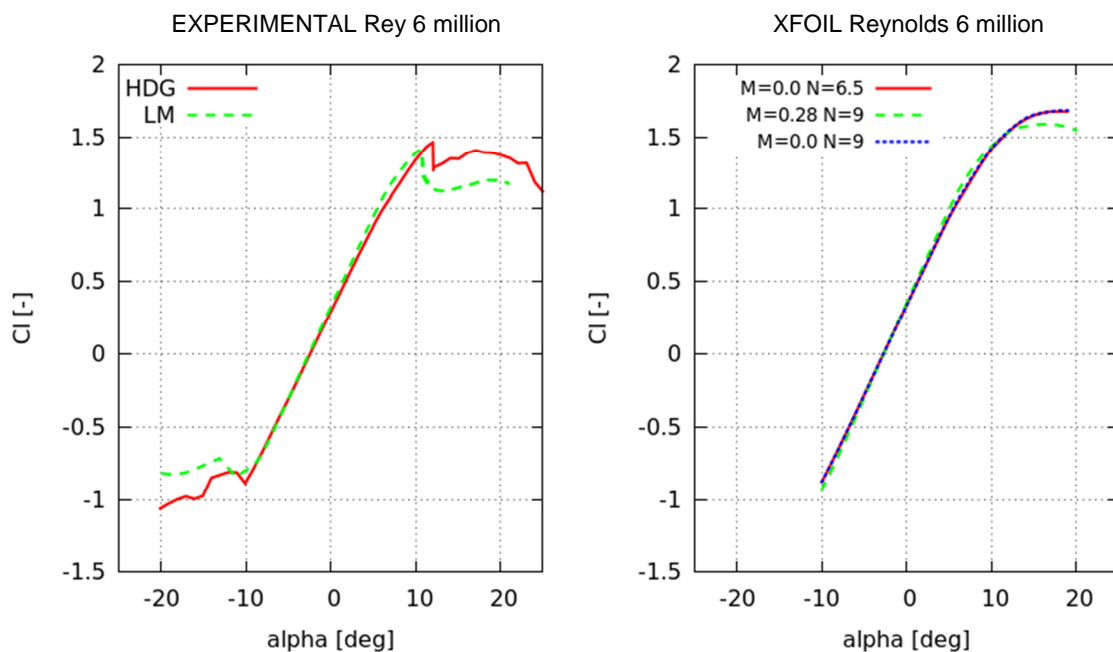


Figure 9. Experimental and XFOIL computations of C_l vs AoA at $Re=6 \cdot 10^6$

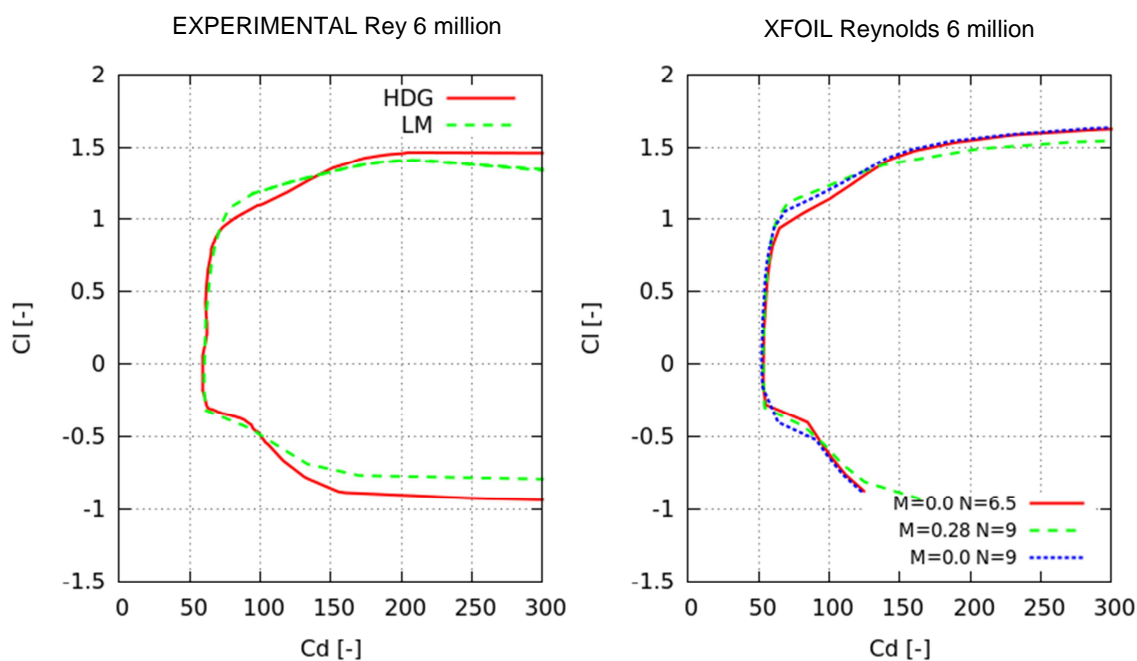


Figure 10. Experimental and XFOIL computations of C_l vs C_d at $Re=6 \cdot 10^6$

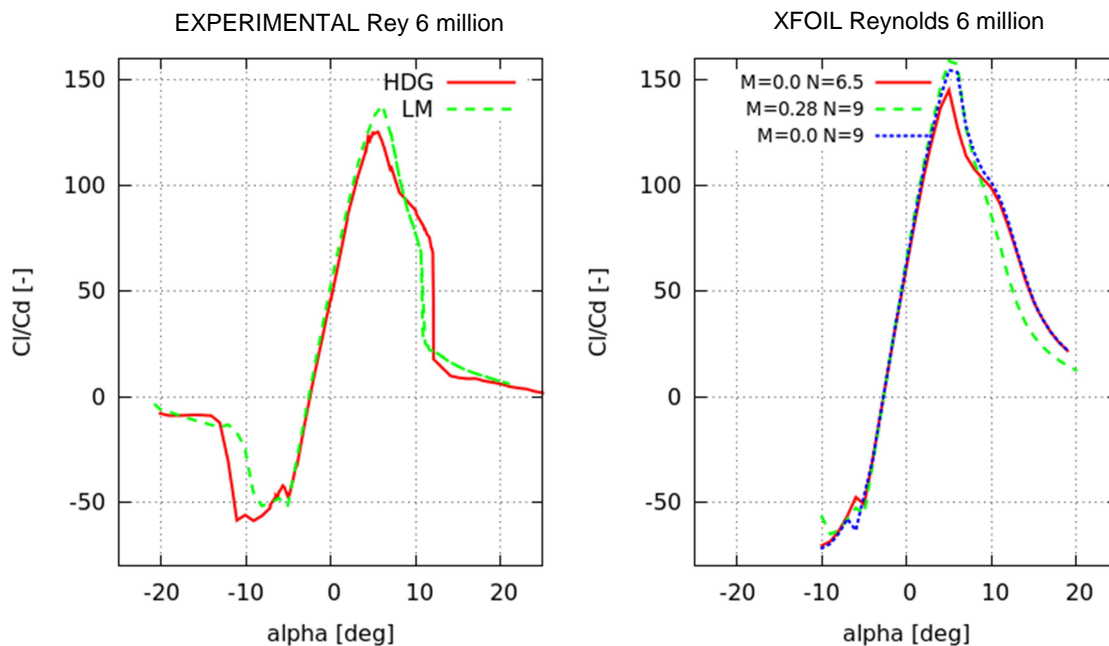


Figure 11. Experimental and XFOIL computations of Cl/Cd at $Re=6 \cdot 10^6$

The XFOIL computations are coherent with the idea that Mach effect influences mainly the lift slope and the different inflow turbulence affects the drag, especially at separation. The right plot in Figure 9 shows how XFOIL predicts a negligible effect of the turbulence (different N -factor values) in lift, while the Mach effect would introduce an increase of the lift slope. On the other hand, Figure 10 shows how turbulence effect has more influence on the drag. Finally, Figure 11 shows the efficiency, which represents the combined effects of lift and drag.

In all of these last three curves, when we compare the left (experimental) plot against the right (XFOIL computation) plot, we can see that the qualitative variations of the aerodynamics coefficients between HDG and LM test are the same as the ones computed with XFOIL. Then the different values at 6 million Reynolds can be explained with the different wind conditions in each wind tunnel.

5. Conclusions

The comparison of the data obtained at 3 million Reynolds number condition at the two different wind tunnels shows a very good agreement. Only differences are shown at stall conditions, which can be explained by the 3D effects caused by the different facilities set-up.

The comparison between data at 6 million Reynolds number shows more significant differences. An analysis of these differences has been performed and the conclusion is that they are consistent with the different Mach number and turbulence intensity in both wind tunnels at this Reynolds number condition.

References

- [1] Schepers G J et al 2016 Latest results from the EU project AVATAR: Aerodynamic modelling of 10 MW wind turbines. Science of Making Torque 2016
- [2] Ewald B F R 1998 Wind Tunnel Wall Corrections. AGARD-AG-336
- [3] Pires O et al 2016 Analysis of high Reynolds numbers effects on a wind turbine airfoil using 2D wind tunnel test data. Science of Making Torque 2016
- [4] Glauert H 1928 The Effect of Compressibility on the Lift of an Aerofoil. *Proc. Roy. Soc. London*. VOL. **CXVIII**, 1928, p. 113–119
- [5] Schewe G 2001 Reynolds-number effects in flow around more-or-less bluff bodies *J. Wind Eng. & Ind. Aerodyn.* **89** 1267-1289
- [6] Llorente E et al 2014 Wind Tunnel Tests of Wind Turbine Airfoils at High Reynolds Numbers *J. of Phys.: Conf. Series* **524** (2014) 012012